International Journal of Pharmaceutics 421 (2011) 1–11

Contents lists available at SciVerse ScienceDirect

International Journal of Pharmaceutics

journal homepage: www.elsevier.com/locate/ijpharm

Towards crystal engineering via simulated pulmonary surfactant monolayers to optimise inhaled drug delivery

Michael J. Davies[a,b,*], Linda Seton[a,b], Nicola Tiernan[a], Mark F. Murphy[a], Paul Gibbons[a]

[a] The School of Pharmacy and Biomolecular Sciences, Liverpool John Moores University, Liverpool L3 3AF, UK
[b] LJMU Institute for Health Research, Liverpool John Moores University, Byrom Street, Liverpool L3 3AF, UK

ARTICLE INFO

Article history:
Received 20 June 2011
Received in revised form 2 September 2011
Accepted 8 September 2011
Available online 16 September 2011

Keywords:
Crystal engineering
Inhaled drug delivery
Langmuir monolayers
Atomic force microscopy (AFM)
Theophylline

ABSTRACT

Purpose: To generate theophylline monohydrate crystals underneath Langmuir monolayers composed of material expressed at the alveolar air–liquid interface. Such monolayers can act as nucleation sites to direct crystallisation. The approach offers a novel route to rationally engineer therapeutic crystals and thereby optimise inhaled drug delivery.
Methods: Langmuir monolayers consisting of either dipalmitoylphosphatidylcholine (DPPC) or a surfactant mix reflecting pulmonary surfactant were supported on an aqueous theophylline (5.7 mg/ml) subphase. The monolayers were compressed to surface pressures reflecting inhalation and exhalation (i.e. 5 mN m^{-1} or 55 mN m^{-1}) with a period of 16 h to allow crystallisation. Analysis involved scanning electron microscopy (SEM), atomic force microscopy (AFM) and powder X-ray diffraction (PXRD).
Results: Condensed isotherms were acquired, which signified surfactant–theophylline interaction. Theophylline monohydrate crystals were obtained and exhibited needle-like morphology. SEM and AFM data highlighted regions of roughened growth along with smooth, stepwise growth on the same crystal face. The surfactant monolayers appeared to influence crystal morphology over time.
Conclusions: The data indicate a favourable interaction between each species. The principal mechanism of interaction is thought to be an ion–dipole association. This approach may be applied to generate material with improved complementarity with pulmonary surfactant thus enhancing the interaction between inhaled drug particles and internal lung surfaces.

1. Introduction

Over the course of recent years drug delivery to the lung has attracted significant interest due to the potential to treat a wide range of both local and systemic disease states (Corcoran, 2006; Arnolds and Heise, 2007). As a result, attention has focussed on refining the solid state of inhaled formulations in an attempt to optimise pulmonary delivery; leading to the generation of engineered, nano-sized and modified release particles (Schiavone et al., 2004; Bhavna et al., 2009; Learoyd et al., 2009). Although this is the case, it would appear that to date, limited consideration has been given to the nature and extent of interaction between inhaled formulations containing active pharmaceutical ingredients (APIs) and pulmonary fluid (i.e. pulmonary surfactant and the supporting hypophase) (Davies et al., 2009). As pulmonary fluid is both the initial point of contact for a drug particle upon delivery to the deep lung and the media in which dissolution takes place, it would seem prudent to investigate the association of these materials fully to improve current understanding of the association between each species.

During drug delivery to the lung, an aerosol formulation must initially negotiate through the tortuous respiratory tract and subsequently associate with and dissolve in surfactant rich pulmonary fluid to liberate the API and thereby achieve the desired effect. If this process is slow, or inhibited in any way, the effectiveness of the preparation may be reduced. Clearly, the association between the inhaled API and pulmonary surfactant is a key stage in drug delivery to the body and as such may dominate the efficacy profile of the compound. If the nature of the chemical and physical interactions between drug and surfactant were better understood, it would raise the potential to engineer inhaled formulations such that the interaction profile is optimised leading to enhanced drug release over time.

A thorough understanding of API solid state properties is crucial in order to achieve favourable material performance during product manufacture and patient use. Consequently, considerable attention has focussed on the crystallisation behaviour and physicochemical characteristics of APIs in order to select for the most suitable

* Corresponding author at: The School of Pharmacy and Biomolecular Sciences, Liverpool John Moores University, Liverpool L3 3AF, UK. Tel.: +44 0151 231 2024; fax: +44 0151 231 2170.
E-mail address: m.davies1@ljmu.ac.uk (M.J. Davies).

0378-5173/$ – see front matter © 2011 Elsevier B.V. All rights reserved.
doi:10.1016/j.ijpharm.2011.09.004

solid form (i.e. polymorphs, hydrates, salts and co-crystals) (Aulton, 2001). The term polymorphism relates to the capacity of a material to exist as two or more crystal forms that demonstrate differences in molecular arrangement within the crystal lattice (Lu et al., 2007). Potential exists for polymorphs of any API to demonstrate differences in physicochemical characteristics, including for example stability, flowability, compression, dissolution, solubility and bioavailability indices (Clas, 2003; Cox et al., 2007). Furthermore, opportunity may present for solid material to transform from one form to another, either during processing or on storage. Hydrates and solvates can equally express different properties and the most desirable form must be selected for formulation. Naturally, issues such as these are of great importance because they may have a significant bearing on the way in which a formulation handles during all stages of processing and end use. The significance of solid-state characterisation and control of API crystal form is therefore widely recognised.

A range of approaches may be exploited to engineer the solid state of an API, including for example the use of polymeric materials (Caruso, 2001), supercritical fluids (Reverchon et al., 2008), self-assembled monolayers (Lee et al., 2002; Cox et al., 2007) and Langmuir monolayers (Loste et al., 2003; Lu et al., 2007). A Langmuir monolayer is a two-dimensional, amphiphilic-based ensemble that may serve as an epitaxial surface to aid the nucleation and growth of organic/inorganic substances dissolved within a supporting subphase (Choudhury et al., 2002; Lu et al., 2007). Upon compression Langmuir monolayers exhibit an ordered structure and thereby offer scope to stimulate crystal nucleation and growth (Frostman and Ward, 1997). Previous work has highlighted the fact that by tailoring the physicochemical properties of the monolayer, the crystallisation of the substrate can be controlled (Lu et al., 2008).

It is evident that this mode of crystallisation is governed by lattice matching (Lu et al., 2001, 2007) and thermodynamic parameters (Rodriguez-Hornedo and Wu, 1991; Lee et al., 2002). By careful selection of appropriate amphiphilic material, Langmuir monolayers may be utilised to simulate pulmonary surfactant at the air–liquid interface as per the arrangement within the alveolar space in the deep lung (Bringezu et al., 2003; Davies et al., 2009).

Pulmonary surfactant is a complex phospholipid–protein blend that covers the internal surfaces of the lower respiratory tract and alveoli (Piknova et al., 2002). This material serves to reduce interfacial surface tension, thereby permitting effective lung function and preventing alveolar collapse (Notter, 2000; Zasadzinski et al., 2001). By doing so, the species exhibits variable surface pressure with respect to respiratory function (Davies et al., 2009). Pulmonary surfactant is primarily composed of saturated dipalmitoylphosphatidylcholine (DPPC), unsaturated phosphatidylcholines and phosphatidylglycerols (i.e. 1-palmitoyl-2-oleyl-sn-glycero-3-phosphatidylglycerol (POPG)) (Bringezu et al., 2003) along with the surfactant proteins SP-A, SP-B, SP-C and SP-D (Goerke, 1998). A deficiency of this material may lead to respiratory distress syndrome (RDS), a condition frequently observed in neonates (Ding et al., 2003); with medical signs including poor gaseous exchange and reduced lung compliance (Notter, 2000). The condition is routinely managed by exogenous lung surfactant preparations (i.e. Survanta®) that are often supplemented with palmitic acid (PA) (Banerjee and Bellare, 2001).

This study aims to investigate the influence of simulated pulmonary surfactant monolayers on the crystallisation behaviour of the bronchodilator theophylline. Here, we intend to assess the physicochemical properties of drug crystals formed within an environment representative of the deep lung. To achieve this, Langmuir monolayers will be employed to simulate pulmonary surfactant monolayers and allow for changes in surfactant phase properties via compressing to pre-defined surface pressures (i.e. to replicate the nature of the internal surfaces of the lungs at the points of inhalation and exhalation).

Theophylline has been chosen as the model compound for study because it is used extensively within the clinical setting to manage acute severe asthma along with chronic obstructive pulmonary disease (BNF 60) and has been subject to extensive investigation (Shefter and Higuchi, 1963; Otsuka et al., 1990; Ticehurst et al., 2002; Cox et al., 2007; Wikstroem et al., 2008). Theophylline is known to exist as four anhydrous polymorphs (i.e. polymorphs I, II, III and IV) along with a monohydrate form (Suzuki et al., 1989; Ebisuzaki et al., 1997; Matsuo and Matsuoka, 2007; Seton et al., 2010). The monohydrate exists as a monoclinic structure with space group $P2_1/n$ in which the theophylline molecules form hydrogen-bonded dimers, joined via contacts with associated water molecules; the unit cell parameters for this API are: $a = 4.468$ Å, $b = 15.355$ Å, $c = 13.121$ Å, $\beta = 97.792^\circ$ and $z = 4$ (Sun et al., 2002). With respect to anhydrous theophylline, the most prevalent form is Form II which crystallises from organic solvents at room temperature or is produced by water loss of the monohydrate. Form II is enantiotropic with Form I (Legendre and Randzio, 2007), which is produced by heating Form II, and slowly converts to the thermodynamically stable Form IV by solvent mediated transformation (Seton et al., 2010).

2. Materials and methods

2.1. Materials

Anhydrous crystalline theophylline, 3,7-dihydro-1,3-dimethyl-1*H*purine-2,6dione, was obtained from Sigma, UK (BN: 056K0686). The molecular structure of theophylline is detailed in Fig. 1.

The crystal habit of theophylline monohydrate was elucidated via the Bravais–Friedel–Donnay–Harker (BFDH) method (Bennema, 1995). The crystal structure data for theophylline monohydrate (Ref: THEOPH01) (Sun et al., 2002) was obtained from the Cambridge Crystallographic Structural Database (Allen, 2002) and the morphology calculation performed using Mercury 2.4 software. The three-dimensional crystal habit for the monohydrate form of the API is presented in Fig. 2.

The surfactants DPPC (Avanti Polar Lipids, USA. BN: 160-181PG-113), POPG (Avanti Polar Lipids. BN: 160PC-286) and PA (Sigma–Aldrich, UK. Ref: P0500) were of analytical grade and used as supplied. The molecular structures of each species are presented in Fig. 3. DPPC is a prevalent, amphiphilic molecule found within the lower respiratory tract and alveolar regions of the lung. This species is zwitterionic and includes a number of oxygen atoms along with methyl and methylene moieties within the structure that are

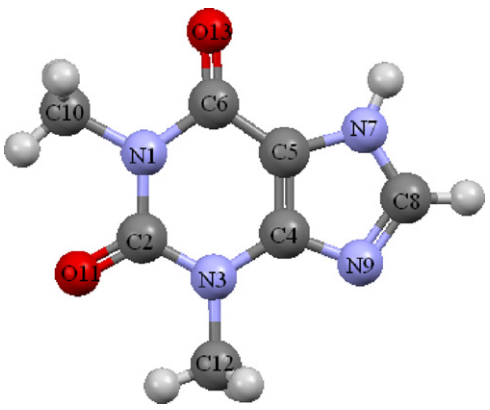

Fig. 1. The chemical structure of theophylline.

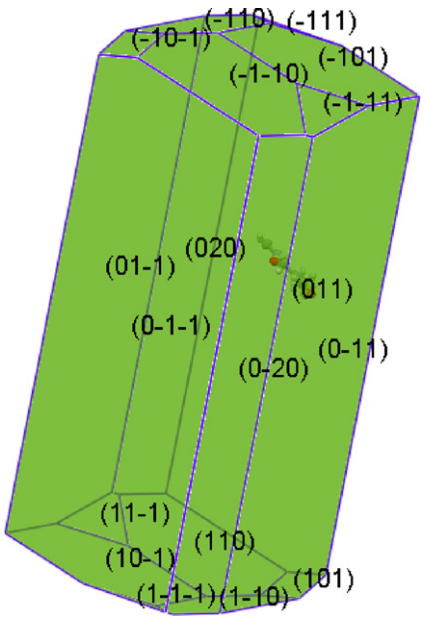

Fig. 2. Predicted morphology of theophylline monohydrate via the BFDH method.

capable of serving as hydrogen bond acceptors and donors, respectively (Minones et al., 2002).

Chloroform ($CHCl_3$) (Sigma–Aldrich, UK) employed as the spreading solvent was of analytical grade (≥99.9%). Ultrapure water (Elga, UK), demonstrating a resistivity of 18 MΩ cm, was used both during cleaning procedures and as the aqueous subphase.

2.2. Methods

2.2.1. Batch crystallisation

Samples of theophylline monohydrate crystals were recrystallised by dissolving 1.08 g of the anhydrous starting material in 100 ml ultrapure water heated to 40 °C in a jacketed beaker connected to a circulating water bath (ThermoHaake DC10, USA). The solution was agitated using a magnetic stirrer at 700 rpm. Subsequently, the solution was cooled to 25 °C over 10 min and stirred for a period of 22 h to facilitate crystallisation. In each case, crystalline material was recovered via Buchner filtration and subsequently analysed via scanning electron microscopy (SEM), differential scanning calorimetry (DSC) and powder X-ray diffraction (PXRD).

2.2.2. Langmuir monolayers

Surfactant monolayers were produced using a Langmuir trough (Model 102M, Nima Technology, UK operated by Nima TR516 software). Initially, all contacting surfaces and glassware were thoroughly cleaned using surfactant free Kimtech tissues (Kimtech Science, Kimberly-Clark Professional, 75512, UK) soaked in chloroform. Cleanliness was assured by performing test runs that monitored surface pressure during barrier compression. The surface of the subphase was considered clean when a surface pressure of 0.4 mN m^{-1} or less was recorded at complete barrier compression in the absence of a surfactant monolayer. Surfactant profiles were based on those known to exist in the pulmonary environment; for instance either DPPC or a mixed surfactant system consisting of DPPC, POPG and PA in the ratio 69:20:11 (w/w/w) to reflect the composition of the commercially available pulmonary surfactant replacement preparation Survanta® (Bringezu et al., 2003).

The chosen surfactant material was dissolved in chloroform to produce a spreading solution (1 mg/ml) and 10 μl of this solution were delivered to the surface of the pure water subphase by dropwise addition from a Hamilton microsyringe. A period of 10 min was observed, to allow chloroform evaporation and surfactant spreading. The trough barriers were programmed to move towards the centre of the trough (i.e. to achieve monolayer compression by reducing surface area) at a rate of 10 cm^2 min^{-1}. A Wilhelmy plate (Minones et al., 2002) at the centre of the compartment allowed for plots of surface pressure vs. area per molecule (i.e. Langmuir pressure–area (π–A) isotherm) for each surfactant system at 25 °C.

2.2.3. Recrystallisation beneath Langmuir monolayers

Recrystallisation was conducted using a theophylline containing aqueous subphase (5.7 mg/ml) at pH 7.0 and temperature 25 ± 1 °C. The monolayer was compressed to surface pressures of 5 mN m^{-1} and 55 mN m^{-1} then left to stand for 16 h to facilitate crystallisation.

The crystalline material was carefully recovered from the Langmuir trough and subsequently characterised as per the reference system. A control protocol was established that involved placing an aqueous solution of theophylline (5.7 mg/ml) within the Langmuir trough in the absence of surfactant monolayers and leaving to stand for a period of 16 h.

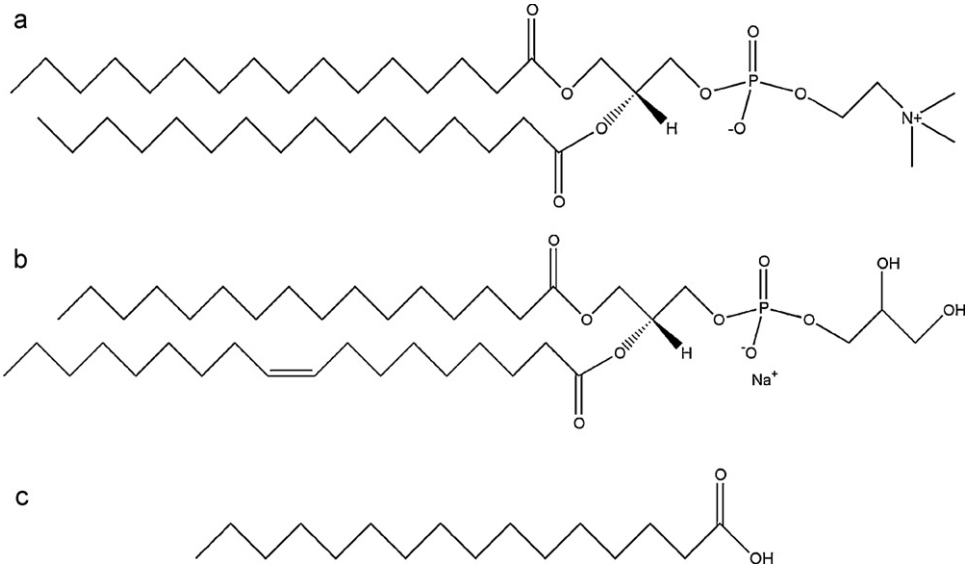

Fig. 3. The molecular structures of (a) DPPC, (b) POPG and (c) PA.

2.2.4. Sample characterisation

2.2.4.1. Differential scanning calorimetry. The solid form of each sample was verified by differential scanning calorimetry (DSC 7, Perkin Elmer Pyris 1, USA). Samples were prepared in hermetically sealed and crimped aluminium pans containing 3–5 mg and scanned over the temperature range 20–285 °C at a rate of 20 °C min^{-1} within a dry nitrogen environment of flow rate 20 ml min^{-1}.

2.2.4.2. Powder X-ray diffraction. Theophylline crystals from each system under investigation were mounted into a zero background sample holder. Powder X-ray diffraction patterns were obtained (Rigaku Miniflex, Rigaku Corporation, Japan) with Cu radiation (λ = 1.54 Å) at a voltage of 30 kV and a current of 15 mA with an automatic, variable divergence slit. Samples were scanned from 5° to 50° 2θ. Patterns were compared with those available in the literature to confirm the solid form (Bennema, 1995; Sun et al., 2002). Data was also collected from unground samples and preferred orientation effects monitored.

2.2.4.3. Scanning electron microscopy. SEM analysis (Quanta 200 SEM, FEI, Holland) was conducted to inspect particle size, gross morphology and surface features of the crystalline material. The samples were initially gold coated using a K550X sputter coater (EMITECH, UK) and subsequently scanned using an acceleration voltage of 10 kV at a working distance of approximately 10 mm.

2.2.4.4. Atomic force microscopy. All images presented were obtained using a Molecular Force Probe-3D (MFP-3D) atomic force microscope (Asylum Research, Santa Barbara, CA) with software written in IGOR pro (Wavemetrics, USA). The MFP-3D is equipped with a 90 μm *x*–*y* scanning stage, *z*-piezo range >16 μm and is coupled to an Olympus IX50 inverted optical (IO) microscope. The MFP-3D-IO was placed upon a TS-150 active vibration isolation table (HWL Scientific instruments GmbH, Germany), which was located inside an acoustic isolation enclosure (IGAM mbH, Germany) to reduce the influence of external noise. The imaging process was executed in contact mode under ambient conditions with v-shaped, silicon nitride cantilevers of nominal spring constant 0.02 N m^{-1} and length 200 μm (OMCL-TR400PSA-1, Olympus). Here, the scan size was 10 μm × 10 μm and imaging parameters including set point, integral gain and scan rate were determined empirically to optimise quality.

2.2.4.5. Molecular visualisation. Using the crystal structure data previously obtained for theophylline monohydrate, surface chemistry was visualised using Mercury 2.4 software. Here, the theophylline functionalities available at exposed solid surfaces were examined.

3. Results

3.1. Langmuir monolayers

Langmuir surface pressure–area (π–A) isotherms were obtained for DPPC and mixed surfactant monolayers supported on both a pure water and a theophylline containing subphase; typical plots are illustrated in Fig. 4 and reflect data described within the literature (Minones et al., 2002; Bringezu et al., 2003). The similarity apparent between each trace indicates that the presence of drug substance within the supporting subphase did not adversely affect monolayer dynamics. It is evident that each plot demonstrates discrete regions (i.e. gaseous (G), liquid expanded (LE), liquid condensed (LC) and solid (S) phases) shown by changes in the gradient of the curve, on flowing right through to left.

Table 1
Theophylline monohydrate yields obtained from various crystallisation environments.

Environment	Yield (mg)
Control: no surfactant monolayer	180
DPPC monolayer 5 mN m^{-1}	82
DPPC monolayer 55 mN m^{-1}	58
Mixed monolayer 5 mN m^{-1}	46
Mixed monolayer 55 mN m^{-1}	87

The limiting area per molecule of DPPC on pure water was approximately 58 Å^2, in agreement with previously reported data (Zhai and Kleijn, 1997; Mu et al., 2005). When the DPPC monolayer was supported on a theophylline containing subphase, a reduced limiting area per molecule was recorded within the region of 50 Å^2. A similar trend was apparent with the mixed surfactant system. The apparent disparity between the plot for pure water and that for aqueous theophylline may be ascribed to the interaction between theophylline molecules in solution and surfactant molecules forming the monolayer structure (Choudhury et al., 2002). The trend is attributed to the binding of drug molecules to the underside of the Langmuir monolayer, in turn forming a condensed ensemble (Mu et al., 2005).

3.2. Generation of samples beneath surfactant monolayers

All crystalline samples nucleated and grew successfully over a period of 16 h. Table 1 shows the yield of theophylline monohydrate crystals obtained from each environment studied. When compared to the control system (i.e. the absence of amphiphilic material) the presence of a surfactant monolayer reduced the observed yield, thus indicating growth inhibition.

This effect was increased significantly for two of the samples, namely the DPPC monolayer at 55 mN m^{-1} and the mixed surfactant monolayer at 5 mN m^{-1}, where there was a reduction in yield of over 70% by weight.

3.3. Differential scanning calorimetry

Each sample exhibited a distinct endotherm in the region of 88 °C (data not shown), attributed to the loss of water from the crystalline structure and confirming the solid form as theophylline monohydrate. No additional phase transitions occurred until the melting endotherm at approximately 276 °C. These data correspond with that previously reported (Cox et al., 2007).

3.4. Powder X-ray diffraction

The PXRD data recorded using the samples obtained agree with that previously reported (Suzuki et al., 1989). Typical PXRD patterns acquired during this work are presented in Figs. 5 and 6.

With respect to the crystalline material recovered from both systems at surface pressures of 5 mN m^{-1} and 55 mN m^{-1}, reflections at 2θ values of 8.8°, 11.4°, 13.2° and 14.5° confirm that the samples are theophylline monohydrate (Suzuki et al., 1989). On inspection of the PXRD data, it is evident that the physicochemical properties of Langmuir monolayers reflecting endogenous surfactant material present at the alveolar air–liquid interface can influence the morphology of theophylline monohydrate crystals. Preferred orientation effects in the unground samples indicate surfaces which are important in the particle morphology. The dominant crystal faces obtained from a DPPC monolayer at 5 mN m^{-1} and 55 mN m^{-1} were (1 0 −3) and (0 2 0), respectively. In the case of the mixed surfactant system the most dominant faces at 5 mN m^{-1} and 55 mN m^{-1} were (0 2 1) and (0 3 5), respectively. The results verify that

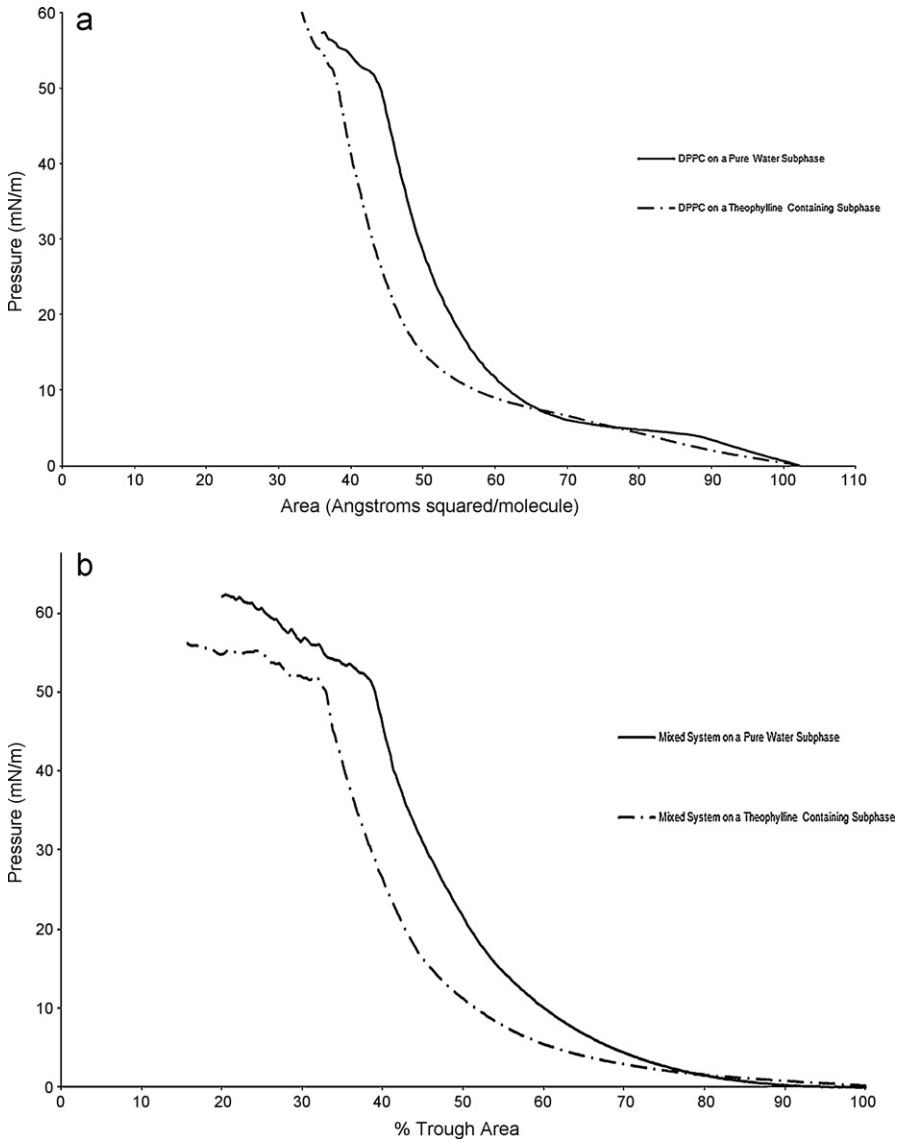

Fig. 4. (a) Langmuir π–A isotherms of DPPC monolayers on a pure water and theophylline containing subphase at 25 °C. (b) Langmuir π–A isotherms of mixed surfactant system monolayers on a pure water and theophylline containing subphase at 25 °C.

the chemical composition of the surfactant monolayer along with applied surface pressure can impinge on crystal morphology, and may indicate differences in the interaction of the monolayer with the growing crystal dependent on these factors.

3.5. Visualisation of crystal surfaces

The dominant crystal faces identified via PXRD analysis were visualised using Mercury v2.4 software; the results are illustrated in Fig. 7. Clearly, there are differences in the surface chemistry

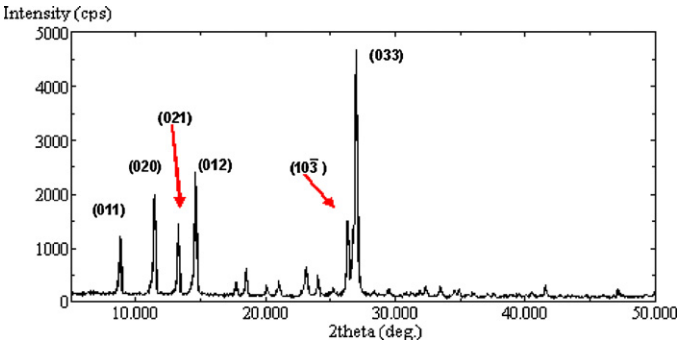

Fig. 5. PXRD pattern of theophylline monohydrate obtained from batch crystallisation post grinding.

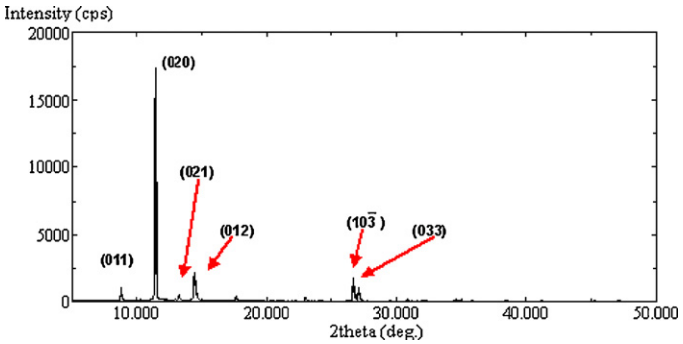

Fig. 6. PXRD pattern of theophylline monohydrate obtained from the DPPC system at 55 mN m^{-1} pre-grinding, showing an increase in intensity in the (0 2 0) reflection.

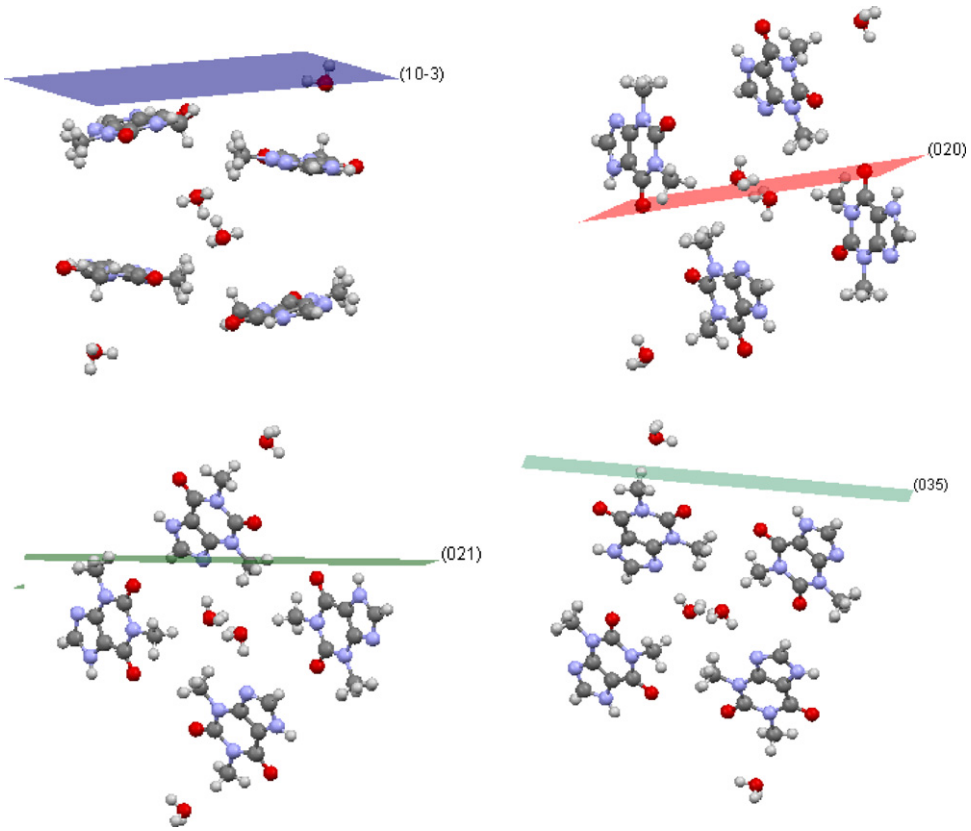

Fig. 7. The organisation of theophylline molecules within drug crystals formed beneath: (a) DPPC monolayer at 5 mN m^{-1} {1 0 −3}, (b) DPPC monolayer at 55 mN m^{-1} {0 2 0}, (c) mixed surfactant monolayer at 5 mN m^{-1} {0 2 1} and (d) mixed surfactant system at 55 mN m^{-1} {0 3 5}. Where light grey represents hydrogen atoms, dark grey indicates carbon atoms, blue signifies nitrogen atoms and red codes for oxygen atoms.

at the faces. The (1 0 −3) surface is parallel to the plane of the molecule and contains the π ring. Interactions at this surface are likely to involve π–π stacking, rather than direct contacts such as H-bonding. This is likely to be a slow growing surface. The (0 2 0) surface contains the C6=O carbonyl function of theophylline, which is electron rich and a hydrogen bond acceptor. This surface grows by forming hydrogen bonds within the structure, leading to relatively fast growth, reflected by its small size within the BFDH prediction shown in Fig. 2. The (0 2 1) surface similarly contains the carbonyl functionality, but also the N–H of the five membered ring as detailed in Fig. 1. The crystal grows at this surface by forming two hydrogen bonds between these groups and their equivalents on a second theophylline molecule. This is likely to result in very fast growth; hence the surface is not featured in the BFDH predicted morphology. The (0 3 5) surface contains the N1–CH_3 and N7–C8H groupings which are likely to form only very weak interactions. This surface is not represented in the BFDH prediction.

3.6. Scanning electron microscopy

SEM analysis revealed that theophylline monohydrate crystals exhibit needle-like morphology (Fig. 8a–f). It is likely that the faces resulting from the BFDH calculation are expressed, but that the relative growth rate in the [1 0 0] direction is fast due to the hydrogen bonding within the structure. The solid material produced under each condition was of comparable size. On inspection at high magnification, the drug crystals displayed variable surface morphology; expressing either reasonably flat regions (i.e. due to stepwise growth) (Fig. 8e) or areas displaying numerous surface undulations which appeared to be secondary microcrystalline particles (Fig. 8f). Of particular note was the fact that several of the SEM images confirmed a mixture of smooth and rough surfaces along the same crystal face (Fig. 8c). In addition, crystal fines featured across particle lengths and larger crystalline particles were found to be distributed across the surfaces (Fig. 8d–e), this result being suggestive of a cohesive nature for the material.

The number of fines was greater in the case of the material produced via Langmuir monolayers, indicating a potentially brittle nature. Such fragmentation is likely to have occurred on removal of the material from the Langmuir trough.

SEM visualisation highlighted variation in the aspect ratio. For example, the crystalline material formed beneath the DPPC monolayer at a surface pressure of 5 mN m^{-1} (Fig. 8c) demonstrated a low aspect ratio, being truncated and wider in comparison to other samples; thus indicating inhibition of growth along the fastest growing direction. With respect to the alpha factor, some samples were significantly roughened (i.e. indicating a low alpha factor) (Fig. 8d), which usually occurs under conditions of high supersaturation or when growth sites are blocked as in the case of a structural additive (Davey and Garside, 2000). However, other samples showed surfaces with planar growth steps (Fig. 8c), suggestive of both a high alpha factor and slow growth over time; generally associated with low supersaturation, or significant poisoning of a growth surface.

3.7. Atomic force microscopy

Typical AFM images detailing the surface morphology of crystalline theophylline monohydrate formed under variable conditions are presented in Fig. 9. The data agree with SEM analysis. On inspection, it is likely that two distinct modes of crystal growth govern the development of the solid material over time; namely, surface nucleation (Fig. 9a) and step-wise growth (Fig. 9c). The

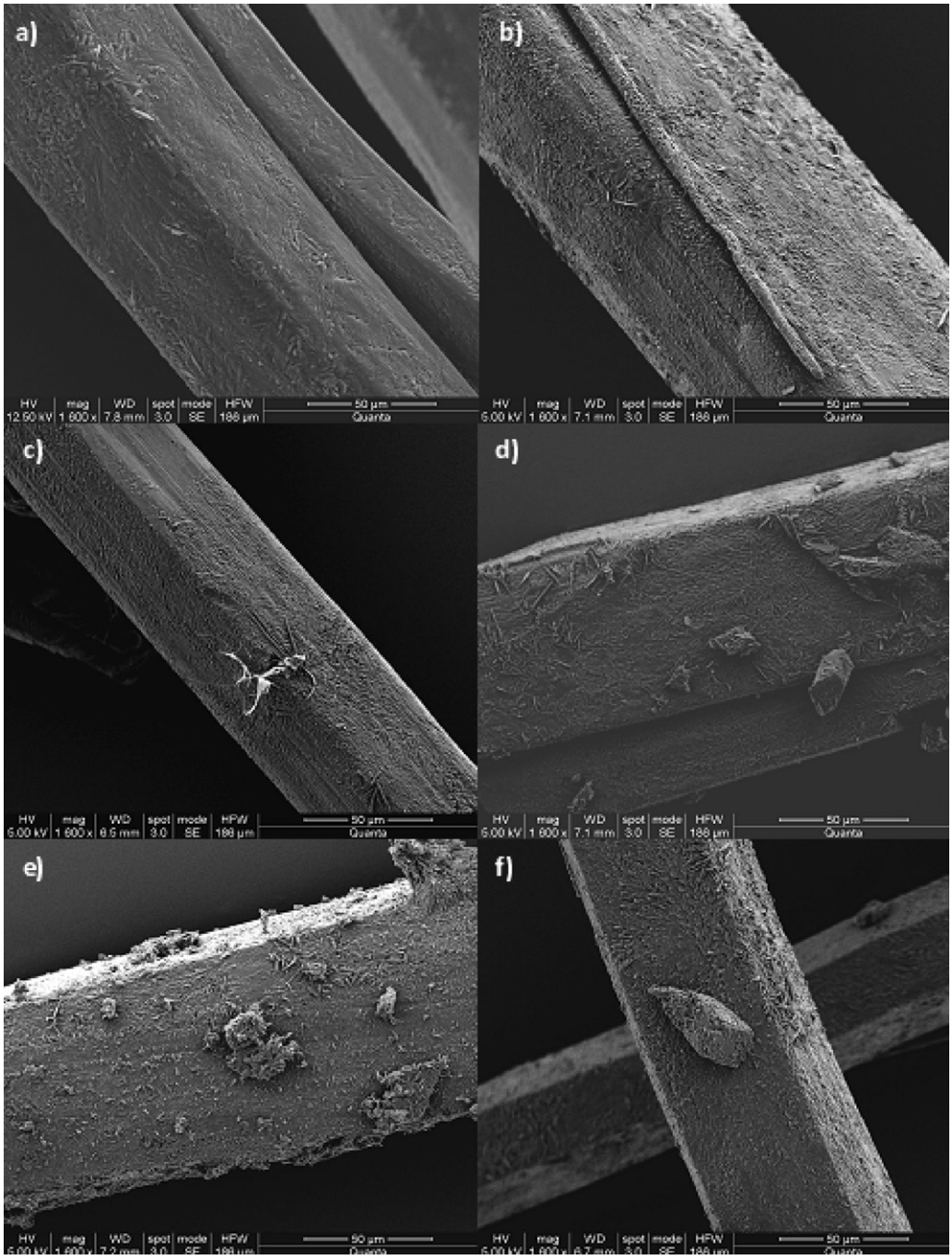

Fig. 8. SEM images of crystalline theophylline monohydrate: (a) batch crystallisation, (b) Langmuir trough with no monolayer, (c) DPPC monolayer at 5 mN m^{-1}, (d) DPPC monolayer at 55 mN m^{-1}, (e) mixed monolayer at 5 mN m^{-1} and (f) mixed monolayer at 55 mN m^{-1}.

combination of such growth patterns results in a number of 'mixed' regions of the solid material exhibiting both relatively smooth morphology and rugosity at the nanoscale (Fig. 9b). It is interesting to note that on analysis such variation was apparent across the entire length of an individual drug crystal (i.e. topography was not homogenous over an entire crystal surface, as exemplified in Fig. 9b). This may result from variation in molecular organisation within the surfactant monolayer or from changes to solid solution composition during growth.

With respect to sample morphology, AFM data highlight the fact that macroscopic surfaces tend to be more roughened as the surfactant surface pressure is increased from 5 mN m^{-1} to 55 mN m^{-1}, as demonstrated in Fig. 9c and f. This result may be explained by considering the fact that surfactant monolayers enter the more ordered solid phase following surface compression (i.e. the constituent molecules become more tightly packed), potentially leading to more effective structural matching and more effective influence on crystal growth. Comparable trends in surface topography were apparent in the case of the mixed surfactant system at surface pressures of 5 mN m^{-1} and 55 mN m^{-1} (note: examples of representative morphology presented, all data not shown).

4. Discussion

The findings presented within this preliminary study confirm that simulated pulmonary surfactant monolayers can influence the

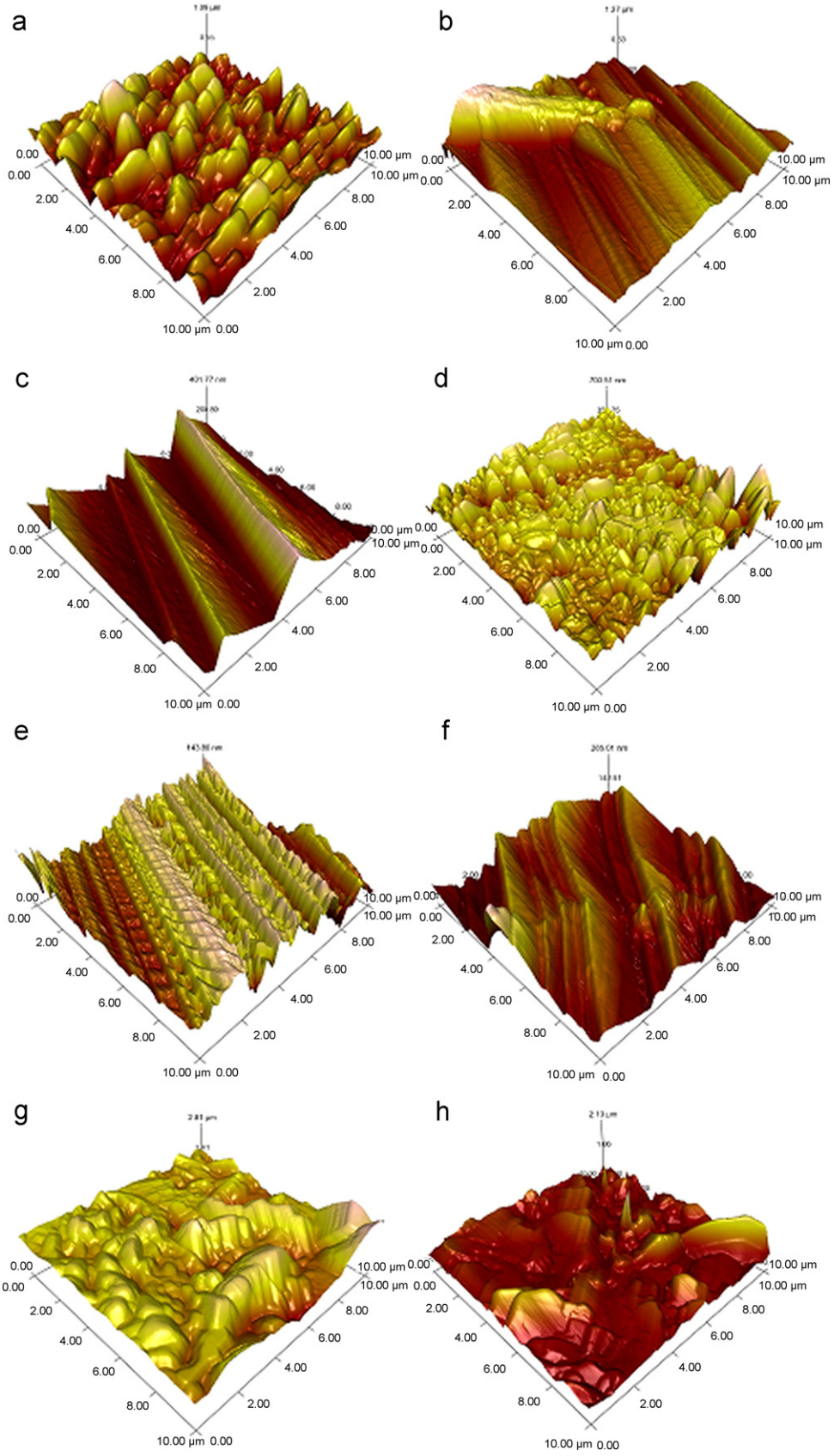

Fig. 9. AFM 3D images of crystalline theophylline monohydrate formed under variable environmental conditions. (a–c) DPPC monolayer at 5 mN m^{-1}. (d–f) DPPC monolayer at 55 mN m^{-1}. (g) Mixed monolayer at 5 mN m^{-1}. (h) Mixed monolayer at 55 mN m^{-1}.

growth and development of theophylline monohydrate crystals over time. Here, we have shown that a model drug substance dissolved within a supporting aqueous subphase does interact with surfactant monolayers at the air–liquid interface, in turn forming condensed molecular ensembles. The data verify that variation in surfactant characteristics can direct the expression of crystal planes, surface chemistry and even influence resultant particle morphology; all of which are key factors for concern in the delivery of therapeutics to the lung.

It is widely recognised that formulation parameters need to be carefully considered and tightly controlled when delivering a therapeutic agent to the body via the pulmonary route (i.e. aspects for reflection include particle size, shape, surface energetics and critically the exposed surface chemistry). On delivery to the deep lung, the initial point of contact for an inhaled drug particle is pulmonary surfactant. Clearly, the interacting chemistry between each species will have a huge impact upon the dissolution profile and hence drug release from the respirable particles. We suggest, therefore, that in order to maximise the degree of interaction between each species it would be desirable to rationally generate respirable material that chemically complements endogenous pulmonary surfactant, with physicochemical changes during the inhalation/exhalation cycle in mind.

If particles could be engineered to comprise the surfaces for which dissolution is favoured, then particle dissolution might be faster or more effective.

The data presented here highlight the application of Langmuir monolayers to achieve just this. Monomolecular films exhibit various chemical groupings that are available for interaction with molecules dissolved in the supporting aqueous subphase. With respect to this study, key associations between simulated surfactant monolayers and the model therapeutic compound include ion–dipole, hydrogen bonding and van der Waals interactions. The availability of binding sites across the two-dimensional surfactant templates allows for an increase in the local concentration of drug molecules when compared to the bulk, thus reducing the activation energy for crystal nucleation and resulting in the development of solid crystalline particles (Xue et al., 2009). Clearly, intramolecular interactions such as these lend themselves to controlling the orientation of drug molecules and initiating nucleation.

It is accepted that simulated surfactant monolayers experience an increase in molecular order in response to an increase in the applied surface pressure (i.e. there is a transition from the 'gaseous phase' through to the 'solid phase' on application of lateral pressure) (Lu et al., 2001; Davies et al., 2009). As the surface pressure is ramped, those theophylline molecules in solution that are proximal to the monolayer experience enhanced molecular order and consequently mimic an arrangement reflecting the native crystal structure. At particular surface pressures, potential exists for the functional groups within the monolayer to structurally match the arrangement of the respective crystal surface, thus leading to crystal nucleation and the expression of a particular crystal face. In this way, there may be specificity to a particular crystal surface and inhibition of that face during growth, leading to its expression in the final particle morphology.

A sound understanding of the chemical composition of the surfactant monolayer is pivotal in order to predict crystal development with respect to time. For example, a surfactant monolayer formed solely from DPPC would be homogenous and exhibit a regular array of component molecules. At low surface pressures, the polar head group of the DPPC molecule (i.e. the phosphorylcholine and glycerol components) is believed to penetrate deep into the aqueous media (Minones et al., 2002). As the applied surface pressure is increased, the head groups become more ordered and are directed towards the air–liquid interface (Minones et al., 2002), thus resulting in variation in the two-dimensional arrangement of the monolayer in response to applied surface pressure. Dependent on applied lateral pressure, the charged ammonium moiety may advance into the bulk solution and therefore attract dissolved drug molecules exhibiting either negatively charged moieties or dipole moments (Mu et al., 2005).

The prominence of the charged ammonium species, in comparison to the phosphate anion, within the bulk solution could potentially lead to an ion–dipole association with theophylline molecules (i.e. ammonium species–carbonyl functionalities) (Lu et al., 2007) thus coding for a particular orientation with respect to the monolayer structure. It is evident that the (0 2 0) surface contains the C6═O carbonyl functionality of theophylline, which is electron rich and a hydrogen bond acceptor. Therefore, at this surface scope exists for hydrogen bond formation with the NH_3 group of DPPC along with the OH groups of POPG and PA. Whilst at a surface pressure of 55 mN m^{-1}, the (0 2 0) surface appeared to be more important in crystal morphology; with growth being inhibited, leading to reduced yield. When the monolayer was exposed to a constant low surface pressure, this effect was not observed.

The scenario with the mixed surfactant system (i.e. DPPC, POPG and PA) is somewhat different. In this case, the amphiphilic material is randomly distributed in a two-dimensional format across the air–liquid interface with various molecular species penetrating into the bulk solution to variable depths. The POPG molecule is structurally similar to DPPC and contains a charged phosphate moiety as exemplified in Fig. 3b.

However, there are terminal hydroxyl groups available within POPG that are capable of forming hydrogen bonds with neighbouring molecules in solution. As per DPPC, variable penetration depths into the supporting subphase are anticipated for POPG at different surface pressures.

Furthermore, the PA molecule, illustrated in Fig. 3c, has a short chain length and single carboxylic acid functionality. This molecule may form only hydrogen bonds with drug molecules in solution. Therefore, the two dimensional array of the mixed monolayer will be less regular when compared to the DPPC monolayer alone, leading to different types of functionality available for interaction. In addition, structural matching might be less effective resulting in variation in nucleation or inhibition effects when compared to the single surfactant system. With respect to the crystal structure of theophylline monohydrate, the (0 2 1) surface contains a carbonyl functionality along with the N7–H grouping of the five membered ring, illustrated in Fig. 1.

The N–H moiety is a hydrogen bond donor and has potential to interact with the P═O and C═O functionalities within for example the POPG and PA molecules. For samples grown under a mixed surfactant monolayer in the gaseous phase, this face was inhibited, indicating a mixture of interactions with the different functionalities present. Furthermore, the (0 3 5) surface contains the N1–CH_3 and C8–H groupings which are likely to form only weak interactions. This particular surface grows by forming hydrogen bonds with the water molecule. This indicates that the interactions formed by the deeper penetration of the surfactant head group into pulmonary fluid at low surface pressures may be important in the dissolution of drug material on the lung surface.

In terms of the control experiments, similar protocols were adopted. In the absence of surfactant material crystals did develop with a much greater yield. Although the morphology appeared similar, PXRD traces indicated that preferred orientation effects were not observed and importantly there was no selectivity for crystal surfaces. The result confirms that simulated surfactant monolayers both reduced crystal yields and selectively inhibited the growth of certain faces, as previously reported (Lu et al., 2007).

The data presented within this study demonstrate that there is favourable chemical interaction between the model compound theophylline and simulated pulmonary surfactant monolayers. The

nature of this interaction is dependent on the chemistry of the API and the composition/compression status of the simulated pulmonary surfactant monolayer. When considering the dissolution of particulate material within pulmonary fluid, it seems likely then that engineering the crystal surface chemistry to optimise the interaction with the surfactant and also the supporting media, might improve the rate of drug release.

Respirable particle manufacture within the pharmaceutical industry may involve for example milling or unit operations such as spray drying (Aulton, 2001). If the surface chemistry were to be tailored in such a way as to complement the internal surface of the deep lung, then clearly the particulate material would need to be preserved in order to present favourable chemistry to that pulmonary surface on delivery. Although Langmuir monolayers present as an attractive means by which to generate crystalline material demonstrating complementarity with pulmonary surfactant, the technique does not lend itself well to the generation of large crystal yields; with typically milligrams of material recovered. Here, the major limiting factor is the area/volume over which crystallisation can take place and the fact that the large crystals of high weight will not be effectively supported by the monomolecular layer.

The reduction of processing during pharmaceutical manufacture is advantageous as it reduces costs and as a result research is underway to develop methods for the direct production of particles suitable for inhalation, such as via microfluidic reactors (Ali et al., 2009) and antisolvent crystallisation (Xie et al., 2010). Antisolvent crystallisation is a technique that allows for the generation of micron-sized drug particles by the addition of a second solvent in which the substrate has low solubility. This causes rapid nucleation and subsequent generation of a large number of small particles. This approach has been utilised to generate salbutamol sulphate particles within the respirable range (Xie et al., 2010). During the process surfactant molecules were successfully used to influence the physicochemical properties of the final product.

The results of this study demonstrate that there is a selective interaction between pulmonary surfactant and specific faces of theophylline monohydrate crystals, which is dependent on monolayer chemistry and surface pressure. This may be applied to improve dissolution within the pulmonary environment. Moreover, potential exists to use surfactants during manufacturing to alter crystallisation outcomes, for example in combination with the addition of an antisolvent. Overall, this substantiates the viability of the crystal engineering strategy highlighted here. Naturally, this approach has the potential to be applied more generally to a number of therapeutic agents. The inhaled route of drug delivery has received increasing attention in recent years not just for treatment of pulmonary conditions but also for a variety of systemic conditions (i.e. diabetes).

To underscore the practical advantage in combining the approaches outlined above (i.e. rational crystal design with appropriate scale up), it is useful to consider both the accepted inhaler technique and the related pathway taken by inhaled drug particles on inhalation. At the outset, the patient is advised to attempt regular shallow breathing cycles and when comfortable activate their inhaler whilst inhaling sharply. The patient should then hold their breath to allow for particle sedimentation to the deep lung. During breath holding pulmonary surfactant within the alveolar space will be in the gaseous phase and expressing a particular chemistry.

As the engineered therapeutic material descends into the deep lung and alveolar space, the initial contact will be with the pulmonary surfactant in that gaseous phase. The particle will locate itself on the surface of the surfactant monolayer and consequently interact with the immediate chemistries. An optimal chemical arrangement will facilitate the improved association between each species and may lead to enhanced dissolution/solubilisation, when compared to conventional products. Once in solution the drug molecules may readily stimulate extracellular receptors, pass into cells to stimulate intracellular receptors or move through into the systemic circulation to exert the desired effect.

In the rational design of API products for inhaled drug delivery, it would appear important to select for the most physiologically relevant formulation with consideration given to lung surfactant characteristics during initial contact.

5. Conclusion

This study has demonstrated that compressed and uncompressed (i.e. as per the inhalation cycle) surfactant monolayers composed of material expressed at the air–liquid interface may influence the crystallisation of theophylline monohydrate. Potential exists to take advantage of this approach to rationally generate therapeutic crystals for drug delivery via the inhaled route. The availability of a two-dimensional array of surfactant molecules, as per the deep lung, may be exploited to elucidate the faces involved for optimal interaction with the *in vivo* scenario. It is possible that the strategy presented within this study could be applied to a range of inhaled formulations to improve the strength and specificity of the interaction at the solid–surfactant interface and develop inhaled formulations demonstrating improved interaction profiles and therefore enhanced drug release.

Further work to widen the presented concepts is planned (i.e. investigating the influence of time and pH on crystallisation via this route along with modelling pulmonary surfactant–drug particle interaction). We hope that that on the development of the principles presented, inhaled formulations displaying improved complementarity with pulmonary surfactant monolayers will be achievable, thus improving the interaction profile of existing inhaled formulations and thereby optimising the management of both local and systemic disease states.

Acknowledgements

The authors would like to thank The School of Pharmacy and Biomolecular Sciences at Liverpool John Moores University for supporting this research effort. In addition, we would like to express our gratitude to Mr. Moazzam Ali for his contribution to early phase development of this work.

References

Ali, H.S.M., York, P., Blagden, N., 2009. Preparation of hydrocortisone nanosuspension through a bottom-up nanoprecipitation technique using microfluidic reactors. Int. J. Pharm. 375, 107–113.
Allen, F.H., 2002. The Cambridge Structural Database: a quarter of a million crystal structures and rising. Acta Crystalogr. B58, 380–388.
Arnolds, S., Heise, T., 2007. Inhaled insulin. Best Pract. Res. Clin. Endocrinol. Metab. 21, 555–571.
Aulton, M.E., 2001. The Science of Dosage Form Design, second ed. Churchill Livingstone, United States of America.
Banerjee, R., Bellare, J.R., 2001. Comparison of in vitro surface properties of clove oil-phospholipid suspensions with those of ALEC, Exosurf and Survanta. Pulm. Pharmacol. Ther. 14, 85–91.
Bennema, P., 1995. Morphology of crystals: past and future. In: van der Eerder, J.P., Bruinsma, O.S.L. (Eds.), Science and Technology of Crystal Growth. Kluwer Academic Publishers, Norwell, MA, pp. 149–164.
Bhavna, Ahmed, F.J., Mittal, G., Jain, G.K., Malhotra, G., Khar, R.K., Bhatnagar, A., 2009. Nano-salbutamol dry powder inhalation: a new approach for treating bronchoconstrictive conditions. Eur. J. Pharm. Biopharm. 71, 282–291.
BNF 60: British National Formulary 60, 2010. British Medical Association & Royal Pharmaceutical Society of Great Britain.
Bringezu, F., Pinkerton, K.E., Zasadzinski, J., 2003. Environmental tobacco smoke effects on the primary lipids of lung surfactant. Langmuir 19, 2900–2907.
Caruso, F., 2001. Nanoengineering of particle surfaces. Adv. Mater. 13, 11–22.
Choudhury, S., Bagkar, N., Dey, G.K., Subramanian, H., Yakhmi, J.V., 2002. Crystallization of Prussian blue analogues at the air–water interface using an octadecylamine monolayer as a template. Langmuir 18, 7409–7414.

Clas, S.D., 2003. The importance of characterizing the crystal form of the drug substance during drug development. Curr. Opin. Drug Discov. Devel. 6, 550–560.
Corcoran, T.E., 2006. Inhaled delivery of aerosolized cyclosporine. Adv. Drug Deliver. Rev. 58, 1119–1127.
Cox, J.R., Dabros, M., Shaffer, J.A., Thalladi, V.R., 2007. Selective crystal growth of the anhydrous and monohydrate forms of theophylline on self-assembled monolayers. Angew. Chem. 119, 2034–2037.
Davey, R., Garside, J., 2000. From Molecules to Crystallizers: An Introduction to Crystallization. Oxford University Press, Oxford.
Davies, M.J., Brindley, A., Chen, X., Doughty, S.W., Marlow, M., Roberts, C.J., 2009. A quantitative assessment of inhaled drug particle–pulmonary surfactant interaction by atomic force microscopy. Colloids Surf. B Biointerfaces 73, 97–102.
Ding, J., Doudevski, I., Warriner, H.E., Alig, T., Zasadzinski, J.A., 2003. Nanostructure changes in lung surfactant monolayers induced by interactions between palmitoyloleoylphosphatidylglycerol and surfactant protein B. Langmuir 19, 1539–1550.
Ebisuzaki, Y., Boyle, P.D., Smith, J.A., 1997. Methylxanthines. I. Anhydrous theophylline. Acta Crystallogr. C53, 777–779.
Frostman, L.M., Ward, M.D., 1997. Nucleation of molecular crystals beneath guanidinium alkanesulfonate monolayers. Langmuir 13, 330–337.
Goerke, J., 1998. Pulmonary surfactant: functions and molecular composition. Biochim. Biophys. Acta 1408, 79–89.
Learoyd, T.P., Burrows, J.L., French, E., Seville, P.C., 2009. Sustained delivery by leucine-modified chitosan spray-dried respirable powders. Int. J. Pharm. 372, 97–104.
Lee, A.Y., Ulman, A., Myerson, A.S., 2002. Crystallization of amino acids on self-assembled monolayers of rigid thiols on gold. Langmuir 18, 5886–5898.
Legendre, B., Randzio, S.L., 2007. Transitiometric analysis of solid II/solid I transition in anhydrous theophylline. Int. J. Pharm. 343, 41–47.
Loste, E., Diaz-Marti, E., Zarbakhsh, A., Meldrum, F.C., 2003. Study of calcium carbonate precipitation under a series of fatty acid Langmuir monolayers using Brewster angle microscopy. Langmuir 19, 2830–2837.
Lu, L., Cui, H., Li, W., Zhang, H., Xi, S., 2001. Selective crystallization of BaF_2 under a compressed Langmuir monolayer of behenic acid. Chem. Mater. 13, 325–328.
Lu, F., Zhou, G., Zhai, H.-J., Wang, Y.-B., Wang, H.-S., 2007. Nucleation and growth of glycine crystals with controllable sizes and polymorphs on Langmuir–Blodgett films. Cryst. Growth Des. 7, 2654–2657.
Lu, F., Zhao, X., Zhou, G., Wang, H.-S., Ozaki, Y., 2008. Control for orientated growth of large size KCl crystals by the competition between spontaneous and induced nucleation/growth on a Langmuir–Blodgett film. Chem. Phys. Lett. 458, 67–70.
Matsuo, K., Matsuoka, M., 2007. Solid-state polymorphic transition of theophylline anhydrate and humidity effect. Cryst. Growth Des. 7, 411–415.
Minones, J., Patino, J.M.R., Conde, O., Carrera, C., Seoane, R., 2002. The effect of polar groups on structural characteristics of phospholipid monolayers spread at the air–water interface. Colloids Surf. A Physicochem. Eng. Aspects 203, 273–286.
Mu, Y.-D., Xiao, F., Zhang, R.-J., Li, H.-Y., Huang, W., Feng, X.-S., Liu, H.-G., 2005. Effects of pH and surface pressure on morphology of glycine crystals formed beneath the phospholipid Langmuir monolayers. J. Cryst. Growth. 284, 486–494.
Notter, R.H., 2000. Lung Surfactants Basic Science and Clinical Applications. Marcel Dekker Inc., United States of America.
Otsuka, M., Kaneniwa, N., Kawakami, K., Umezawa, O., 1990. Effect of surface characteristics of theophylline anhydrate powder on hygroscopic stability. J. Pharm. Pharmacol. 42, 606–610.
Piknova, B., Schram, V., Hall, S.B., 2002. Pulmonary surfactant: phase behaviour and function. Curr. Opin. Struct. Biol. 12, 487–494.
Reverchon, E., De Marco, I., Adami, R., Caputo, G., 2008. Expanded micro-particles by supercritical antisolvent precipitation: interpretation of results. J. Supercrit. Fluids 44, 98–108.
Rodriguez-Hornedo, N., Wu, H.-J., 1991. Crystal growth kinetics of theophylline monohydrate. Pharmaceut. Res. 8, 643–648.
Schiavone, H., Palakodaty, S., Clark, A., York, P., Tzannis, S.T., 2004. Evaluation of SCF-engineered particle-based lactose blends in passive dry powder inhalers. Int. J. Pharm. 281, 55–66.
Seton, L., Khamar, D., Bradshaw, I.J., Hutcheon, G.A., 2010. Solid state forms of theophylline: presenting a new anhydrous polymorph. Cryst. Growth Des. 10, 3879–3886.
Shefter, E., Higuchi, T., 1963. Dissolution behaviour of crystalline solvated and nonsolvated forms of some pharmaceuticals. J. Pharm. Sci. 52, 781–791.
Sun, C.Q., Zhou, D.L., Grant, D.J.W., Young, V.G., 2002. Theophylline monohydrate. Acta Crystallogr. E58, O368–O370.
Suzuki, E., Shimomura, K., Sekiguchi, K., 1989. Thermochemical study of theophylline and its hydrate. Chem. Pharm. Bull. 37, 493–497.
Ticehurst, M.D., Storey, R.A., Watt, C., 2002. Application of slurry bridging experiments at controlled water activities to predict the solid-state conversion between anhydrous and hydrated forms using theophylline as a model drug. Int. J. Pharm. 247, 1–10.
Wikstroem, H., Rantanen, J., Gift, A.D., Taylor, L.S., 2008. Toward an understanding of the factors influencing anhydrate-to-hydrate transformation kinetics in aqueous environments. Cryst. Growth Des. 8, 2684–2693.
Xie, S., Poornachary, S.K., Chow, P.S., Tan, R.B.H., 2010. Direct precipitation of micron-size salbutamol sulphate: new insights into the action of surfactants and polymeric additives. Cryst. Growth Des. 10, 3363–3371.
Xue, Z.-H., Dai, S.-X., Hu, B.-B., Du, Z.-L., 2009. Effect of Langmuir monolayer of bovine serum albumin protein on the morphology of calcium carbonate. Mater. Sci. Eng. C 29, 1998–2002.
Zasadzinski, J.A., Ding, J., Warriner, H., Bringezu, F., 2001. The physics and physiology of lung surfactants. Curr. Opin. Colloid Interface Sci. 6, 506–513.
Zhai, X., Kleijn, J.M., 1997. Molecular structure of dipalmitoylphosphatidylcholine Langmuir–Blodgett monolayers studied by atomic force microscopy. Thin Solid Films 304, 327–332.